

## Design and analysis of solar-powered VTOL aircraft system for surveillance

Isha Likhite<sup>1</sup>, Sadhvi Chaubey<sup>2</sup>, Sakshi Kolekar<sup>3</sup>, Yogini Chaudhari<sup>4</sup>

<sup>1</sup>Department of Mechanical Engineering, Sardar Patel College of Engineering, Mumbai, India

<sup>2</sup>Department of Mechanical Engineering, Sardar Patel College of Engineering, Mumbai, India

<sup>3</sup>Department of Mechanical Engineering, Sardar Patel College of Engineering, Mumbai, India

<sup>4</sup>Department of Mechanical Engineering, Sardar Patel College of Engineering, Mumbai, India

\*\*\*

**Abstract** - UAVs today are used for a variety of applications, from recreational aviation to advanced world defense. Aside from a host of applications, modern UAVs are plagued by the age-old problem of limited range, due to battery power. Studies have suggested that more energy is used between the vertical departure phase and the arrival phase. To reduce this, the potential solution can be used in the form of VTOL UAVs introduced into the air. This may reduce the energy lost during direct and indirect climbs and this effectively increases the range. Along with this using a solar powered aircraft will take us towards a sustainable option. In this paper, we did the analysis, calculations and market research of the propulsion system and proposed the best combination of electronics required for the successful flight of a UAV. The design and evaluation of a wing are presented in this paper with combination of solar and battery power. We also aimed at building a vertically launching aircraft to save power. The presented wing is capable of producing a lift of 7kg and can be used for a surveillance aircraft.

**Key Words:** solar-powered, VTOL, aircraft, lift, drag, payload, surveillance

### 1. INTRODUCTION

Solar-powered aircrafts use solar rays to fly. As an ideal airline, a solar aircraft uses sunlight as a source of power, which helps to avoid the burden of conventional oil in the air, detect long journeys, replace disrupted communications in different natural disasters; fly over the Storm, track and see the storm; can also go and check the enemy in a predetermined area for a long time, directing the target of the aircraft. It, therefore, has broad operational prospects in both military and commercial camps. Vertically taking off aerial vehicles because of their ability to straighten and sit down drew more attention and their ability to travel at high speeds, thus presenting wide operational prospects. Considering the flexibility and versatility of applications in areas with limited or narrow spaces, our design introduces a compact tri-copter configuration tilt-rotator airplane with full flight paths from rotor mode to a conventional mode and vice versa. A multi-input multi-output, non-affine, multi-channel cross-coupling, and indirect system can be created from an inert air tilt-rotor using a variety of methods. As a result, we decided to create a photovoltaic tilt rotor aircraft.



Fig- 1: Boeing Solareagle

AtlantikSolar, the first updated UAV solar project, was led by Oettershagen et al. of the Autonomous Systems Lab at the Swiss Federal Institute of Technology Zurich. The UAV set a new world record after completing an 81-hour flight covering 2,338 km. With just a wing of 5.69 m span and an overall weight of 6.93 kg, it features a standard rowing configuration. The new method arose from a venture to develop solar-powered UAVs that could fly constantly with solar energy in the finest of weather conditions. The project started with modeling a robust system to take into account variations in working conditions and weather conditions. The airframe and power generation system and storage were designed according to the parameters found in the dynamic system model. Parts of the power machine, like Maximum Power Point Trackers (MPPT) and battery management system, were customized and could control the flow of energy and provide detailed energy flow information. The plane controlling system was developed with models from the earth's atmosphere. With the completion of the flight plan design, the design of the entire UAV was pre-confirmed with lab testing and short-flight testing.



Fig- 2: AtlantikSolar

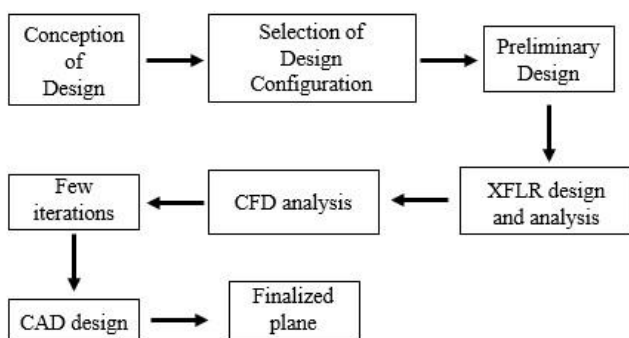
The next solar-powered UAV model was developed by Morton et al. at the University of Minnesota's Center for Distributed Robotics. A solar UAV with a wingspan of 4m was developed for moderate aerial hearing applications. A regular trip in that Vehicle was determined to require plus or minus 46 W of energy. It had a maximum output of 180 W. Solar energies that are more than 300% of the power required for a basic flight. The airframe was designed to accommodate the utilization of low-level air sensing devices. The force needed for such a level of aircraft was calculated using the airframe's aerodynamic features. Following that, an energy system was designed. Several electrical system elements, like MPPT, were tailor made to meet the requirements of a specific project. The solar energy system is made up of 64 Solar radiation powered C60 photovoltaic cells and a custom-made MPPT with a 91.59% efficiency rate. The aircraft control system was built in accordance with the equipment specifications. The mass of the plane was determined only after design of the flight systems.

## 2. Design Objectives Considered

The aircraft is designed considering the following objectives as specified in the problem statement.

- VTOL capability of the UAV.
- Capable of taking off from a platform of 100 m height.
- Endurance of 90 minutes and maximum take-off weight of 7 kg.
- Surveillance area of 50 km<sup>2</sup>
- Payload up to 0.5 kg
- Service ceiling height of 1000 m.
- Feasible and cost-effective solution.

## 3. Aircraft Modelling Algorithm



## 4. Overall Design of the Aircraft

### A. Basics of the unmanned solar-powered UAV.

The plane will capture solar energy using solar panels, and using the Maximum Power Point Tracker (MPPT), a portion of the power will be retained in the battery, while the remainder will be used to power the airplane's components. At night, the plane only depends on the power preserved in the battery to

maintain the flying ability, or the battery can be taken off and charged for the next flight.

### B. Description of mission

Remotely operated solar-powered planes are primarily used only for reconnaissance, surveillance, image data collection, and other tasks, and are typically outfitted with camcorders, thermal imaging equipment, and so on. Our goal is to inspect a 50-square-kilometer area in 90 minutes.

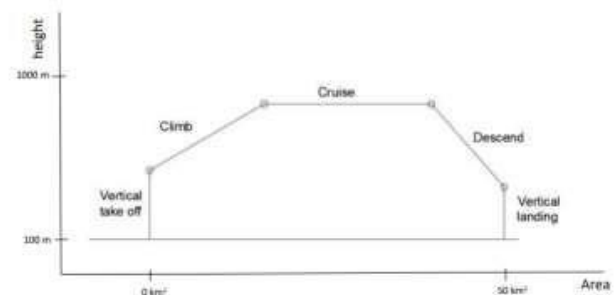


Fig- 3: Mission Profile

- The first stage: more tension force to climb (tentatively uniform speed).
- The second stage: cruise with constant energy supply.
- The third stage: constant descent and later landing.

The photovoltaic propulsion device launches the plane and causes it to take off from a 100 m platform using the remote control. The remote - controlled plane retains its standard altitude of operation after reaching a predetermined peak of about 700m and commences its journey of planned operations. After the mission is completed, the aircraft will transition to a clear landing flight as well as descend mildly. In the mission above:

- Vertical takeoff needs a tension higher than the total of the plane weight, the payload, as well as the resistance.
- Solar-powered plane demands a considerable spread of solar panels and enough power to supply for motor, propellers and also other power facilities.

### C. Possible missions

- During war, if a soldier is injured and he needs medication that is not available at the camp, ALVTOLA can collect the required stuff and deliver it at the war site without landing. Picking and placing mechanism can be developed which will perform the required task.
- Forest Department can use it to keep a watch on the jungle.
- We can place object detectors and smoke detectors in the UAV for quick identification of any required object or find any fire breakouts respectively.
- With significant camouflaging our AL-VTOLA can be used by the military for secret missions, where they need to place cameras or audio devices. It can either drop these devices on multiple locations or can be used as a secret device by itself.
- The Navy can replace the traditional naval fighter jets with AL-VTOLAs as they do not need a runway.
- During calamities like floods, earthquakes, etc. AL-VTOLA can be of great help for supplying food or essentials to the people and for easy identification and rescue.

#### D. Vertical take-Off and landing (VTOL) implementation

Exploring the different types of aircraft configurations and their advantages, disadvantages, and functions have led us to select a Tiltrotor Design configuration that combines the vertical power of a helicopter with the speed and a range of standard aircraft with fixed wings. Also, it is easy to control and move up.

Rotors can be configured to be more efficient in forward flight mode to avoid the issues faced in a helicopter, the plane can reach speeds faster than helicopters. With its rotors upright, they can take off, land, and expand like a helicopter and in the normal flight mode it can fly like a conventional fixed wing plane without compromising the aerodynamic capabilities.

#### E. Select the overall layout of the aircraft

Our primary objective was to employ solar power as an energy source. We designed solar powered VTOL with a good efficiency, portable lithium ion polymer battery as ultimate equipment, high torque for DC motor, and the finest propeller in the driving device. We aimed to select a design that met the design requirements, the most important of which was to use vtol. We used classic design (fully developed technology, design, and process simplification), a greater span to chord ratio (needed for solar aircraft), and a retrofit thrust tilt rotor. Its advantage is that:

- the rotors can be attuned to a required angle of attack to maintain the level flying state as well as obtain reversing thrust
- the assembly is simple.

To achieve this design, three sets of rotors are required: two huge power motor propellers fitted on both ends of a symmetrical wing, and then a tiny power power motor propeller installed in the centre of the fuselage for aircraft balance. The layout diagram is as follows:

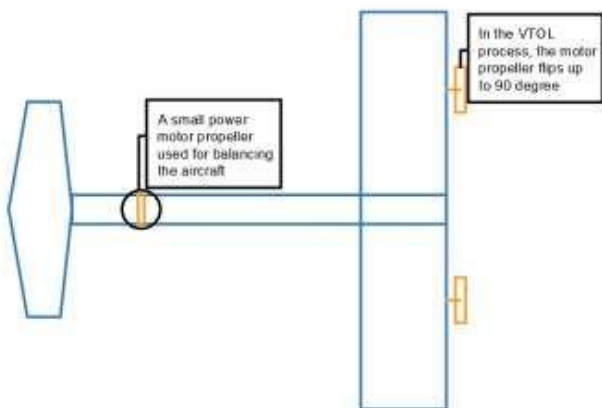


Fig- 4: Overall layout of aircraft

### 5. Detailed Design and Strategy

#### A. Research on the propulsion system

The solar power system has been chosen because unlike the chemical systems, it requires very little weight to accelerate the aircraft. The propellant is released twenty times faster than the old chemical thruster so the whole system works best in bulk. The system consists of a battery, an electronic speed controller, an engine, an MPPT, a propeller, and a transmitter-receiver.

##### a. Solar panel selection:

When light strikes the PV cell, it generates voltage and current. The I-V curve represents the relationship between the amount of sun's energy reaching Earth and the quantity of electricity produced and available energy in a PV cell (Current-voltage curve). The I-V curves of PV cells differ depending on the type and model, but they are very similar. As shown in Fig 5, the I-V curve indicates the voltage-current connection in specific isolation. Also many I-V curves are depicted in the graph to demonstrate the efficiency of a PV cell in different isolation.

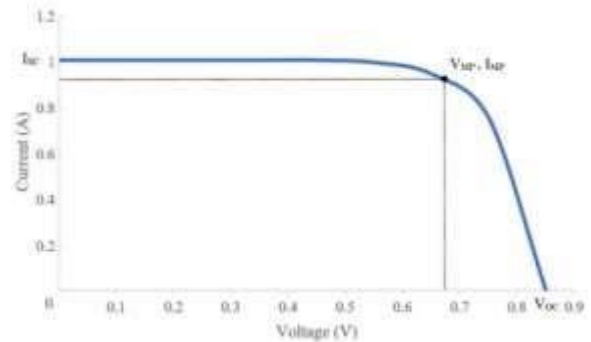


Fig- 5: IV curve

The energy generated by the cell is used entirely to power the solar panels. We chose SunPower C60 monocrystalline silicon solar panels based on their manufacturing cost, utilisation, and maturity level. The SunPower C60 solar cell has a performance somewhere between 21.8% and 22.5%, that is greater than the current monocrystalline silicon cell efficiency of 15% to 20%. Specifications of SunPower C60 solar cell:

- Weight: 0.008kg
- Dimensions: 125mm x 125mm
- Thickness: 16.5mm



Fig- 6: SunPower C60

Given the size and area of both the wings, an average of 24 PV cells have been fitted on the aircraft, 12 across each wing, as

illustrated in Figure 4. The PV cells weigh 0.192 kg in total. A photo Voltaic array was formed by connecting all 24 PV cells in series.

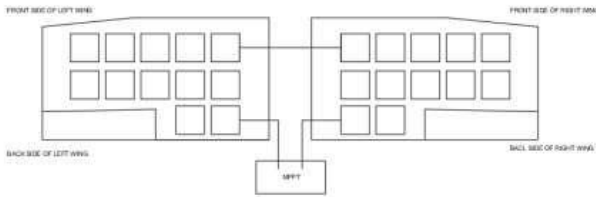


Fig- 7: Placement of solar cells on the wing

According to the manufacturer's data, a single solar SunPower Under radiation from the sun of 300 to 1000 W/m<sup>2</sup>, C60 transmits about 0.5 V. Given that certain PV cells were placed behind the wings, the same PV members were expected to produce a maximum output of less than 12 V.

The aircraft has one PV system. Given that the inclination angle of photovoltaic cells with in wings varies so little, the influence of enhancing the quantity of sunlight radiated individually into various parts of PV is negligible. Individual MPPTs for identical PV members are also not required. Having PV from identical members saves MPPT weight.

### b. Storage Battery

The inbuilt power storage device serves as the second power supply. It should have a high charging efficiency, output capacity, and power density. We chose lithium-ion batteries because of the cost of production, utilization rate, and technical intelligence level associated in our project. Crowding of fuel load is not appropriate as we are developing a prototype of a small UAV. The storage size of a lithium battery, on the other hand, is approximately 110-170Wh / kg, with a power rating of 1000-1200W / kg, which corresponds to the needs of our design. The total current is equivalent to the product of the battery's capacity in mAh and C rating. The battery's current rating should be greater than the maximum peak draw of the motor. If the battery works under maximum current, the life span of the battery will be shortened. Specifications of our battery are as follows:

- Name: Lipo 22000 7s 25.9 V
- Capacity: 22,000 mah
- Cells: 7S
- Voltage rating: 25.9 volts
- Charge: True 40C rating
- Dimensions: 158mm x 59mm x 141mm
- Weight: 2950 g



Fig- 8: Lipo 22000 7s battery

The battery can be charged externally and can be used for a flight when solar power is not available.

### c. Motor selection

A brushless permanent magnet rare metals motor was chosen. Our system design needs were that the plane weigh less than 6 kg, that the load be 0.5 kg, and that the maximum weight in the calculation be 7 kg. In the VTOL system, the motor we chose should be able to lift such a weight. For a classic aircraft design, we select a high-powered rotor with a propeller that provides primary lift, whereas the other small rotor just serves to value the aircraft. As a result, every powerful propeller should produce at least 4 kg of thrust.

The rotational speed of a motor is equal to the output of KV and voltage. When the KV value is high, the torque will be below it. The value of KV affects the choice of the propeller, as a large propeller requires high torque i.e. low KV to rotate. Specifications of our motor are as follows:

- T MOTOR ANTIGRAVITY MN7005 115KV
- Idle current: 0.4 A
- Peak current: 15A
- Internal Resistance: 288 m ohm
- Motor weight: 188g
- Motor size: Ø79 x 21 mm
- Shaft diameter: in 15mm



Fig- 9: T MOTOR ANTIGRAVITY MN7005

### d. Propeller Selection

When an aircraft takes off, accelerates, and begins its journey, we must ensure that it can endure wind resistance, air temperature and pressure, environmental conditions, and so on. A propeller aircraft typically employs a wide range of pitches to alter power. However, in recent years, foreign scientists have adopted a fixed-pitch propeller, that further positions the aircraft better before landing. Vehicle speed variations can result in shortages for some high pitches. We have selected pitch propellers, which can greatly reduce the weight of our aircraft as well as satisfy our design requirements. By looking at the information and adapting to the motor power above, we have selected an electric propeller with the following features:

- Propeller 18x10 CCW 2B E
- Diameter: 457.2 mm
- Pitch: 254 mm
- Bolt diameter: 10mm
- Weight: 52g



Fig- 10: Propeller 18x10

- Power module output: 4.9~5.5V
- Max input voltage: 6V
- Max current sensing: 120A
- USB Power Input: 4.75~5.25V
- Servo Rail Input: 0~36V
- Dimensions: 44x84x12mm
- Weight (plastic case): 33.3g Weight (aluminum case): 49g

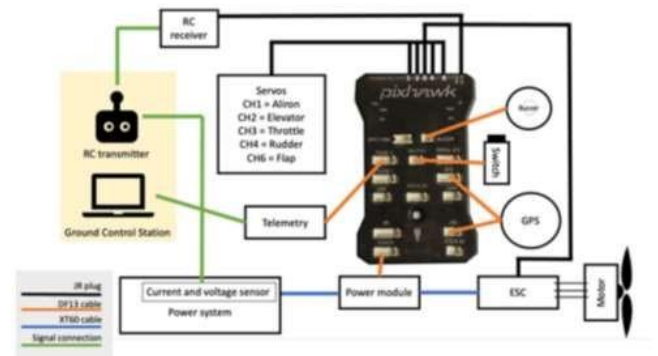


Fig- 12: Autopilot connections

### e. MPPT

Most saliently, an MPPT design that matches the PV system's output voltage and the battery's charging voltage should be chosen. The PV system's total output voltage is predicted to be lower than 12 V, and the voltage needed to charge a 7S LiPo battery is roughly 25 V. Because the total energy of the PV array is inadequate to meet the battery's minimum charging capacity, MPPT should have a voltage boost feature. Another requirement for MPPT selection is proper power conversion. The surplus energy obtained by the PV array could be transmitted to the power system if the MPPT efficiency is high.

Given the above, the MPPT design Genasun GVB-8-Li-28.4V Boost MPPT was chosen for this model.

Specifications of our MPPT are as follows:

- Minimum Panel voltage for charging: 5 V
- Minimum Battery Voltage for Operation: 9.5 V
- Tracking Efficiency: 99%
- Operating Temperature: -40°C – 85°C
- Weight: 185 gm
- Dimensions: 140 x 65 x 31 mm



Fig- 11: Genasun GVB-8-Li-28.4V Boost MPPT

### f. Autopilot System

A few market automated driving models were compared relying on automated driving requirements. Open-source autopilot models were chosen due to their low cost and ease of use in optimising the design element of the UAV flight control system. As a consequence, Pixhawk's legacy was selected because it has features that meet the project requirements at an affordable price. Pixhawk consist of sensors and also an interface that supports and accepts worldwide satellite navigation system (GNSS) signals. It is possible to use an actual kinematic GPS receiver (RTK). A battery discharge circuit module powers all of the components. The details of our Autopilot system are as follows:

### g. ESC selection

There is a current specification for ESCs. The ESC is determined by the dimensions of the propeller as well as the battery. A bigger propeller and battery necessitate a higher ESC value.

Specifications of our ESC are as follows:

- Size: 86.106mm x 39.878mm
- Current Level: 70A
- Burst Current: 80A
- Weight: 150g



Fig- 13: Electronic speed controller

### h. Receiver

S6R (6CH Receiver with built-in 3-axis gyro and 3-axis acceleration). Specifications of our receiver are as follows:

- Dimensions: 47.42 x 23.84 x 14.7mm
- Weight: 12.1 g
- Operating Voltage region: 4.0 V - 10V
- Operating current: 100 mA at 5V



Motor characteristic at full throttle

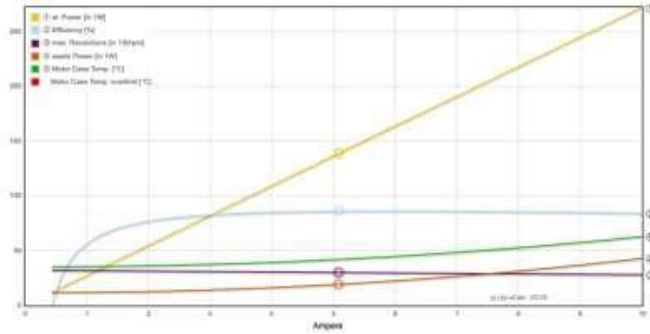


Fig- 18: Motor characteristics at full throttle

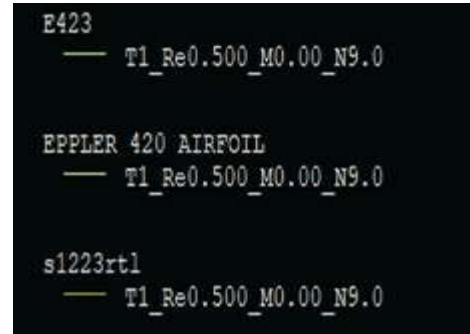


Fig- 20: Xflr airfoils analysed for wing

Sr. No.	Name of airfoil	Cl <sub>max</sub>	α <sub>stall</sub> (deg)	Stall quality	Drag bucket	Cm0	(Cl/Cd) <sub>max</sub>
1.	E420	2.17	14.43	gentle	widest	-0.23	105.425
2.	s1223-rtl	2.39	16.94	gentle	widest	-0.245	83.55
3.	E423	2.03	12.83	gentle	wider	-0.238	123.142

E423 is a good option as it has the highest lift to drag ratio but was rejected due to the narrow drag bucket and lowest maximum lift coefficient. This curtailed the airfoil list to s1223-rtl and e420.

Eppler 420 was selected over s1223-rtl as it offered:

- Lowest minimum drag coefficient
- Higher lift to drag ratio((Cl/Cd) max)
- High lift curve slope
- Structurally enforceable

Although this airfoil does not achieve a Cl<sub>max</sub> of 2.39 like s1223-rtl, it is likely to be easier to build owing to the reduced amount of aft camber as well as greater thickness in the trailing edge region (increase in ease of manufacturability cross-section).

**b. Wing Configuration**

After choosing an airfoil, the wing planform was designed by iteratively varying both the wingspan and chord. For each combination, the resulting configuration was analyzed to determine how the aircraft lift and drag vary with angle of attack, using

$$CL = CL_0 + CL_\alpha * \alpha$$

$$CD = CD_{min} + K * (CL - CL_0)^2$$

A monoplane with high wing configuration was chosen as it provides:

- More flexible use of space inside the fuselage.
- Easy accessibility to the fuselage for loading and unloading of cargo as the area might be dense forest or swamps.
- More ground clearance to avoid ground-level obstacles.
- Protects the wing from high-temperature exit gases in a VTOL aircraft.
- Generates higher lift as compared to the mid and low wing.
- Also, the plane has a lower stall velocity, since CL<sub>max</sub> will be higher.

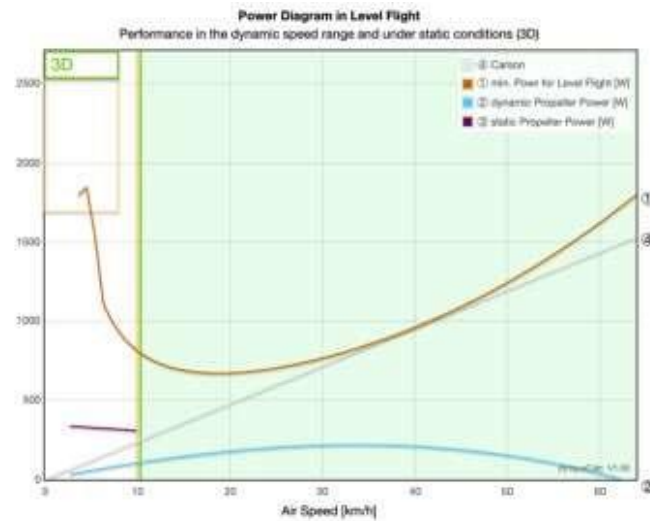


Fig- 19: Performance graph

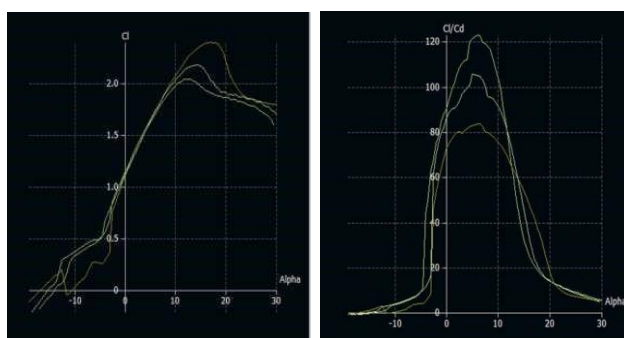
**C. Wing and Aerodynamics**

**a. Airfoil selection**

Several airfoils suited for low Reynolds number regimes like EPPLER 420, s1223rtl, E423 were considered for analysis. Analysis was done for each airfoil at Reynolds Number 5,00,000 by considering factors such as:

- highest maximum lift coefficient (Cl<sub>max</sub>)
- lowest minimum drag coefficient (C<sub>dmin</sub>)
- highest lift-to-drag ratio((Cl/Cd) max)
- lowest (closest to zero; negative or positive) pitching moment coefficient (C<sub>m</sub>)
- proper stall quality in the stall region.

Analysis graphs:



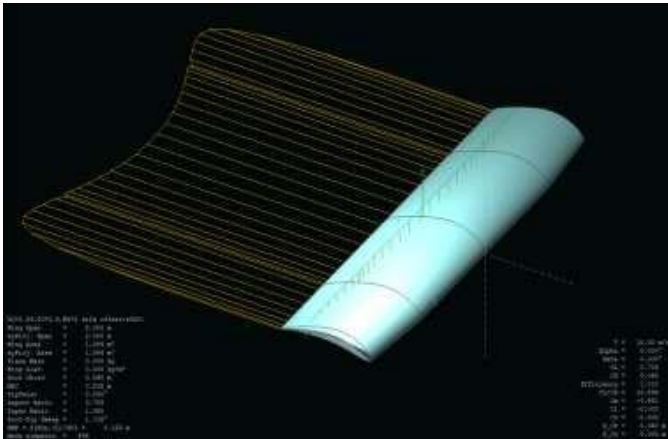


Fig- 21: Wing planform on xflr

The high wing configuration did not require the use of dihedral as it would make aircraft susceptible to Dutch roll.

Wing planform with a straight trailing edge and the tapered leading edge was chosen for better aileron positioning.

Tapered wing planform is selected due to following reasons:

- Better lift distribution.
- Effective at high speeds (as per the mission the aircraft needs to be cruised at high speed).
- Causes an increase in lift and decrease in drag, as reduced drag results in longer flight time.
- Structural benefit due to saving in weight of a wing.
- Lower bending moment at the wing root, as the center of gravity of each wing section (left and right) will move toward the fuselage centerline.

Forward swept planform was chosen because:

- It improves maneuverability.
- Prevents tip stall at a high angle of attack due to airflow from wing tip to wing root.

After doing many iterations, a planform was selected with:

- Higher CL
- Lower CD
- Higher CL/CD
- higher Cm
- Higher aspect ratio

Following are the graphs obtained during XFLR analysis:

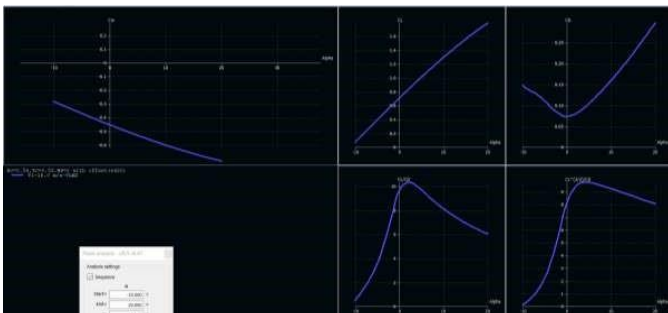


Fig- 22: Xflr graphs for wing

The team selected “Forward swept Straight leading edge” plan form as shown in fig with the following specifications:

Table- 1: Specifications of wing

1.	Aspect ratio	3.759
2.	Taper ratio	1.08
3.	Wing Span	2.00m
4.	Root chord	0.54m
5.	Tip chord	0.5m
6.	Area	1.064m
7.	MAC	0.532m
8.	Cl at alpha=0	0.706
9.	Cd at alpha=0	0.042

**c. Control surfaces (Rolling Moment)**

To determine the size of the ailerons, an initial estimate of 30% of the wing’s chord length was chosen with an aileron span equal to about one-half of the span of each section of the wing. These estimates are based on historical data and based on empirical relations. Hence, ailerons with 70% x hinge and 50% y hinge with 30° flap angle were selected.

The team analyzed different plan forms by considering the following design requirements:

- Less power at cruise
- Less thrust at cruise

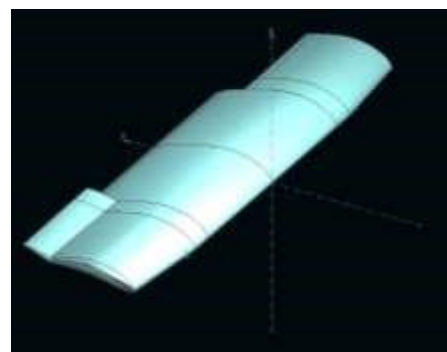


Fig- 23: Ailerons

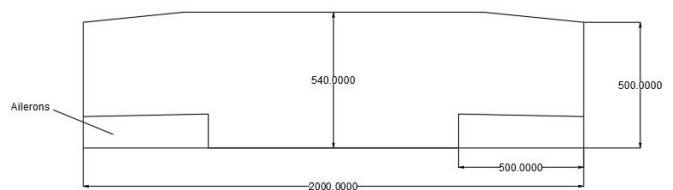


Fig- 24: 2D wing planform

**d. Empennage**

*i. Tail Configuration*

Upon finalizing the wing design, the horizontal and vertical tail parameters were determined considering aircraft stability. As

shown in Figure below, we performed a trade study by investigating six different designs for the tail configuration including a conventional tail, a cruciform tail, a half-H tail, a full Htail, a T-tail, and a V-tail

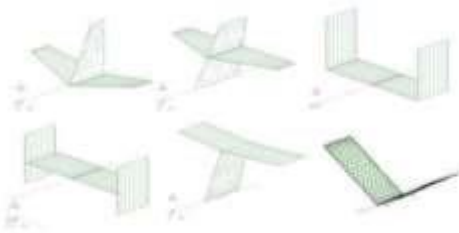


Fig- 25: Trade study for empennage

From our analysis, we quickly removed the V tail due to the additional complexity of the ruddervator configuration required. Also, cruciform is not the best design option because it requires the steering pin to be split or shortened to provide a horizontal stabilization position.

The team has fully evaluated the standard designs, half-H tail, H-tail, and T-tail as our flight options. After some adjustment, we also reduced the selection to the half-H tail and the full H-tail configuration as these designs allow the aircraft to have more power to pull the plane without the extra height commonly required with T. -p tail designs.

Finally, after determining whether the proposed aircraft still had sufficient clearance to rotate when taking off, the team opted for a half-tail H design. With this suspension of the empennage, our aircraft will have enough control power with a little extra length.

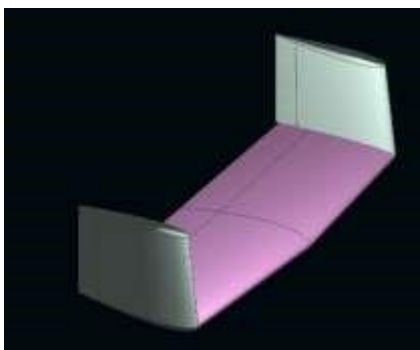


Fig- 26: Empennage

ii. Airfoil selection

To provide a stabilizing moment, the team looked for airfoils that could generate lift with minimum drag and also pitching moment.

Symmetric airfoils were considered so that tail would behave similarly in positive as well as negative AoA.

We chose a larger stall angle over the stall attributes (sharp or docile) of a airfoil so that the horizontal tail will never stall, i.e. the wing will stall before the tail to maintain longitudinal control by using an elevator during such a stall.

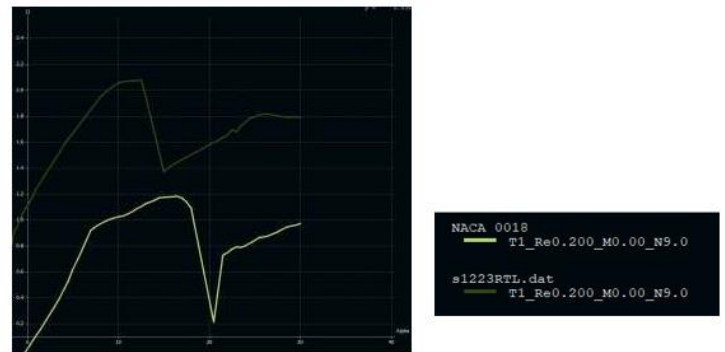


Fig- 27: Airfoil graph analysis for tail

As a result, NACA 0018 was selected which stalls at 16 deg AoA at  $Re = 2 \times 10^5$

We used the volume coefficient method to size both the vertical and horizontal portions of our empennage. The following equation was used to determine the surface area that would be necessary for the aircraft’s vertical stabilizers:

$$S_{VT} = \frac{c_{VT} b_W S_W}{L_{VT}}$$

A similar equation was used to determine the horizontal tail (SHT) area:

$$S_{HT} = \frac{c_{HT} c_W S_W}{L_{HT}}$$

iii. Elevator sizing

Two major functions have been completed here: longitudinal control and also longitudinal trim. Elevator chord was chosen empirically with  $CE / Ch$  (elevator chord to tail chord ratio) = 1/3, implying that elevator chord should be 30% tail chord.

$$CE = Ch / 3 = 0.38 / 3 \approx 0.126 \text{ m}$$

The elevator’s length is selected to be equivalent to the length of the horizontal tail for ease of construction (i.e.,  $bE / bh = 1$ ).

To avoid losing height (flowing over the H.S.), we determined that the maximum deviation of the elevator should be less than or equal to 30 degrees (both up and down). Therefore, the maximum deviation of the elevator is determined by the tail stall requirement.

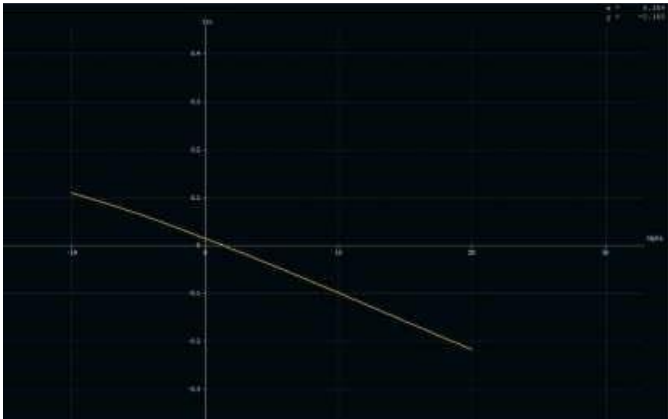


Fig- 28:  $C_{m\alpha}$  graph

iv. Rudder Sizing

Iterative analysis was done on XFLR for various sizes of Vertical Stabilizers. The V.S. dimensions which we choose were analyzed on XFLR with a full rudder deflection of 30°. We got  $C_{n\beta}$  to be 0.17 per radian

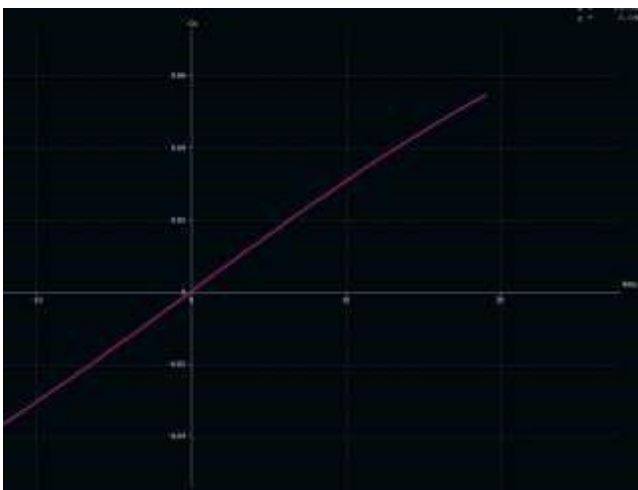


Fig- 29:  $C_{n\beta}$  graph

The specifications for the empennage are shown in table 2

Table- 2: Specifications for tail

1.	Horizontal tail span	1.00 m
2.	Horizontal tail area	0.36 m <sup>2</sup>
3.	Horizontal tail root chord	0.38m
4.	Horizontal tail tip chord	0.34 m
5.	Horizontal tail aspect ratio	2.78
6.	Vertical tail span	0.51m
7.	Vertical tail area	0.17m <sup>2</sup>
8.	Vertical tail root chord	0.35m
9.	Vertical tail tip chord	0.32m
10.	Vertical tail aspect ratio	2.4
11.	Tail Volume	0.72
12.	$C_{m\alpha}$	-0.604 per radian
13.	$C_{n\beta}$	0.17 per radian

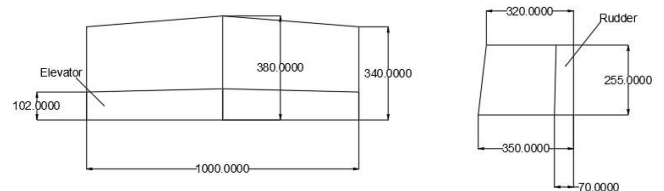


Fig- 30: 2D tail platform

v. Landing Gear

In addition to determining the contact area of our plane, we also explored the aircraft's suspension gear. The main landing gear distance ( $x_{mg}$ ) is calculated below using the total size of the plane and also the resulting value of moment generated. Because we've chosen tricycle landing gear, our plane's elevator must be powerful enough to turn the plane around the main gear and elevate the nose at the rate of an angular pitch. This requirement is met if the aircraft has a take-off velocity of 80% ( $0.8V_{TO}$ ) and when the nose landing gear is in the forward position. This requirement is the rotation at a given angular speed. We assume that the angular acceleration  $\ddot{\Theta}$  is  $5 \text{ deg} / \text{sec}^2$  as our aircraft fits well in the small transport segment as given in the table below.

Table- 3: Angular Accelerations of various planes

No.	Aircraft type	Rotation time during take-off (s)	Take-off pitch angular acceleration (deg/s <sup>2</sup> )
1	Highly maneuverable (e.g., acrobatic GA and fighter)	0.2-0.7	12-20
2	Utility, semi-acrobatic GA	1-2	10-15
3	Normal general aviation	1-3	8-10
4	Small transport	2-4	6-8
5	Large transport	3-5	4-6

Following is the placement of landing gear in our UAV

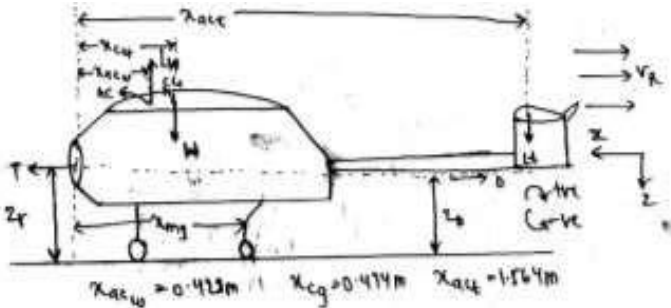


Fig- 31: Landing Gear placements

## 6. Weight Budget

To get a rough weight build-up of various parts of aircraft and to estimate its CG, approximate weight ratios were used based on general UAVs and their components.

Table- 4: Weight Estimation

Component	W/W <sub>to</sub>	Estimated Weight(kg)
Motor 1 (including prop)	0.052	0.34
Motor 2 (including prop)	0.052	0.34
Motor 3 (fuselage)	0.052	0.34
Esc 1	0.023	0.15
Esc 2	0.023	0.15
Esc 3	0.023	0.15
Nose LG	0.012	0.08
Main LG	0.03	0.2
Battery	0.45	2.95
Receiver	0.0018	0.012
Autopilot	0.005	0.033
MPPT	0.028	0.185
Payload	0.077	0.5
Camera	0.007	0.05
Fuselage	0.03	0.2
Wing	0.123	0.8
Empennage	0.077	0.5
<b>Total Aircraft</b>		<b>6.98 + 0.02 (margin)= 7 kg</b>

Solar-powered UAV takeoff weight can be calculated from the following formula:

$$M_{total} = m_{structure} + m_{battery} + m_{propulsion} + m_{load}$$

- $M_{total}$ : aircraft take-off weight which is constant during the flight;
- $m_{structure}$ : aircraft structural weight;
- $m_{propulsion}$ : propulsion system weight;
- $m_{battery}$ : aircraft battery weight, including the weight of solar panels and storage batteries;
- $m_{load}$ : the weight of load

### A. The structural weight

$$m_{structure} = \alpha_1 * m_{total}$$

$\alpha$ : the structural weight coefficient, in our calculation  $\alpha_1=0.23$

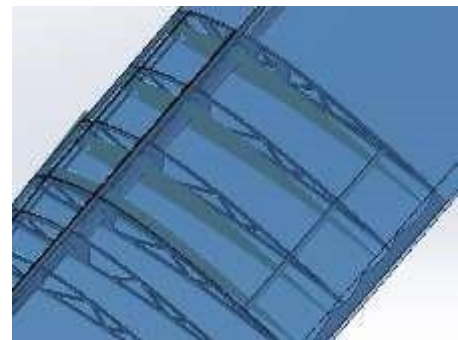


Fig- 32: Skin Design



Fig- 33: Wing Structure

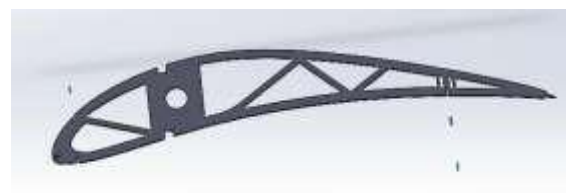


Fig- 34: Wing Rib Design

**B. The propulsion system weight**

The total weight of the propulsion system satisfies the following formula:

$$m_{propulsion} = m_{motor} + m_{ESC} + m_{propeller} + m_{adapter} + m_{receiver} + m_{autopilot} + m_{other}$$

in our calculation:

$$m_{propulsion} = (188*3)g + (52*3)g + (100*3)g + (150*3)g + 12g + 33g = 1.515kg$$

**C. The power battery weight**

$$m_{battery} = m_{storage\ battery} + m_{solar\ panel} + m_{mppt}$$

in our calculation:

$$m_{battery} = 2950g + 192g + 185g = 3.327kg$$

**D. Load**

$$m_{load} = m_{payload} + m_{camera}$$

in our calculation:

$$m_{load} = 500g + 50g = 550g$$

**E. Total weight of aircraft**

According to the above analysis, the aircraft takeoff weight can be expressed as:

$$m_{total} = \frac{m_{propulsion} + m_{battery} + m_{load}}{1 - \alpha_1}$$

Considering the above data, we can calculate the total weight as 7 kg, which meets our design requirements.

**7. Aircraft CG estimation**

Calculation of horizontal and vertical tail parameters which is based on static stability analysis was done by varying the position of wing relative to fuselage. Stability also depends on the position of the wing and CG of the aircraft, so the approximate location of various components as determined in the weight budget was considered. Iterative analysis was done on XFLR5 software for optimum tail moment arm and CG location during forwarding flight mode of operation. Also, CG of aircraft had to be as close to the center of vertical thrust as possible during VTOL mode for stable take-off and landing and to eliminate the need for separate RCS (reaction control system) for balancing excessive pitching moment due to misalignment between CG and center of thrust. (Balancing of vertical thrust for VTOL). Best CG location (fully loaded aircraft) considering thrust balancing and static stability during the forward flight was determined by iterative XFLR analysis.

$$X_{np} = 0.264$$

**A. Placement of components in our aircraft**

Table- 5: C.G. location of components

Component	Estimated Weight(kg)	Location of CG on X-Axis(m)	Location of CG on Y-axis(m)	Location of CG on Z-axis(m)
Motor 1 (including prop)	0.34	-0.05	0.56	0.05
Motor 2 (including prop)	0.34	-0.05	-0.56	0.05
Motor 3	0.34	0.92	0.00	0.05
Esc 1	0.15	0.36	0.56	0.07
Esc 2	0.15	0.36	-0.56	0.07
Esc 3	0.15	0.36	0.00	0.07
Nose LG	0.08	-0.179	0.00	-0.16
Main LG	0.2	0.25	0.00	-0.15
Battery	2.95	-0.02	0.00	-0.48
Receiver	0.012	0.015	0.00	-0.011
Autopilot	0.033	0.051	0.00	-0.012
MPPT	0.185	-0.03	0.00	-0.45
Payload	0.5	-0.159	0.00	-0.04
Camera	0.05	-0.254	0.00	-0.04
Fuselage	0.2	-0.18	0.00	-0.010
Wing	0.8	0.216	0.00	0.044
Empennage	0.5	1.346	0.00	0.02
<b>Total Aircraft</b>	<b>6.98 + 0.02 (margin)= 7 kg</b>	<b>0.181</b>	<b>0.00</b>	<b>-0.010</b>

**B. Static stability**

A plane's static stability is usually the first form of stability which a designer considers when developing a new aircraft configuration. It is a measurement of the relative locations of the centre of gravity (CG) and also the neutral point (NP). XFLR is used to calculate the neutral point, which is a configuration element. If the CG is ahead of the neutral point, a subtle disturbance in the pitch will cause a moment of restoration, eventually returning the aircraft to its initial position and stabilising the configuration. Moreover, if the CG is set too far forward, the plane can be difficult to handle and control is greatly reduced. Static margins are provided by:

$$SM = \frac{X_{NP} - X_{CG}}{MAC} * 100$$

Table- 6: Stability Margin

C.G. (fully loaded)	0.18 m (from the leading edge of the wing)
Neutral Point	0.264 m (from the leading edge of the wing)
Static margin	16.8%

Most aircraft have static margins ranging between 5% and 20%. As a result, this range was selected as suitable for our aircraft. As a result, the devised plane is statically stable in the forward flight.

### 8. Fuselage Design

In general, the length of the fuselage should be 60% of the span length, which is  $L = 2 \text{ m} \times 60\% = 1.2\text{m}$  in our design.

- Initial estimate for the size of fuselage required was done by considering minimum length and height of fuselage required to house payload and other electronics.
- A tricycle landing gear was used for landing on uneven surfaces of remote areas.
- The length of fuselage was kept variable during initial design and was determined based on CG location and tail moment arm obtained from stability analysis.
- Most of the fuselage is optimized for storing maximum payload.
- Payload Bay: We aimed to provide maximum space for the payload with maximum lifting capacity. However, due to the weight constraint, our payload weight was restricted to 500 gm. However, we made a greater space for the payload to accommodate more lightweight items. It was designed for easy loading and unloading of payload without disturbing the CG.

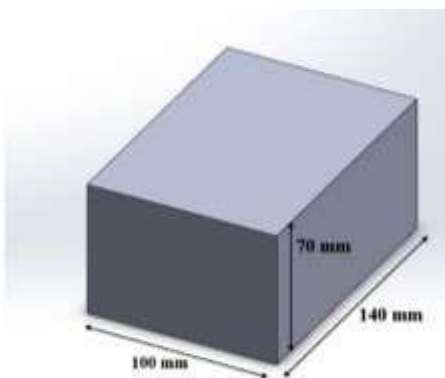


Fig- 35: Payload Bay

- Loading: Payload can be placed from the top as there will be an opening provided to the fuselage.
- Unloading: Payload can be unloaded using the same opening.
- A position for the camera was also determined to get a clear view of the area without any interruption and obstacle.

### 9. CFD Analysis

Following are the various analysis that we performed using Solidworks Flow Simulation. With our detailed CFD analysis we got the exact aerodynamic details of our aircraft.

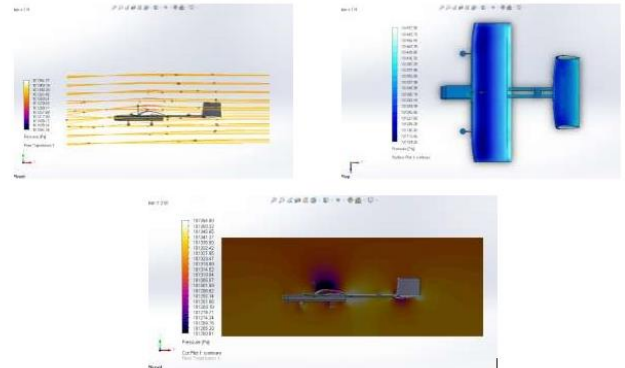


Fig- 36: Pressure Distribution

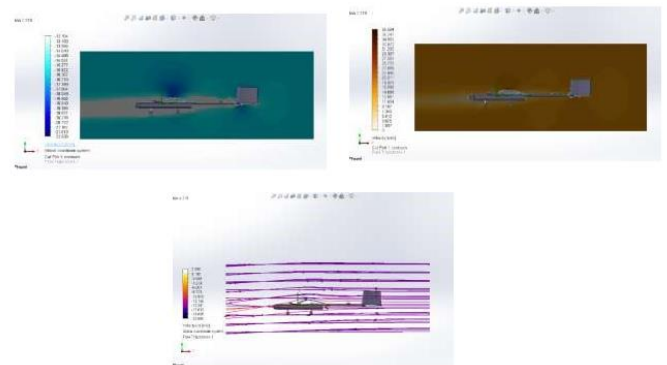


Fig- 37: Velocity Distribution

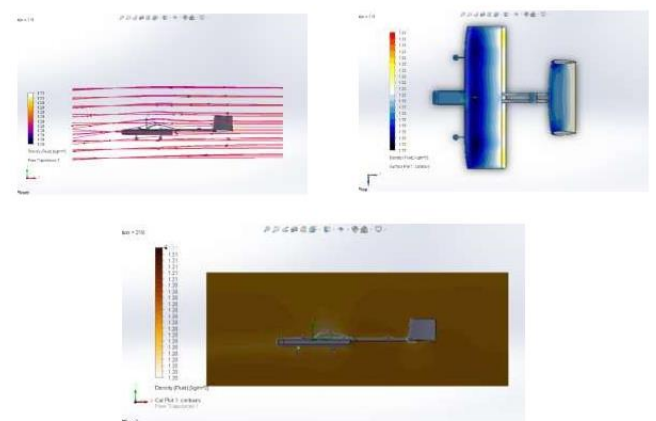


Fig- 38: Fluid Density Distribution

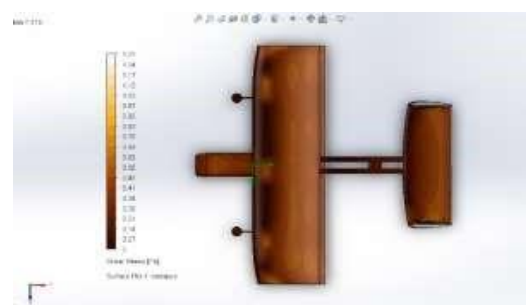


Fig- 39: Shear Stress Distribution

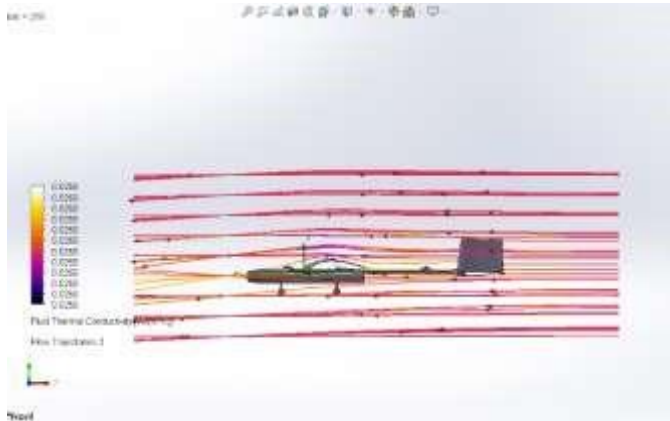


Fig- 40: Fluid Thermal Conductivity Distribution

### 10. Material Selection

We wanted to build a portable but sturdy aircraft, so the stationary components and horizontal tail are made of lighter materials like balsa to save weight, and then other prototype structures are built into the multilayer board.

Double-sided tape can be used to attach PV cells to the wings. A protective coating can be added to shield the cells and guarantee a more secure installation. It can be the covering of a clear sheet of plastic that shrinks when heated. The plastic film can be first applied to the wings using super glue, covering all PV cells; it is then blown with a hot air gun, shrinking to follow the bend of the wing. The image below represents a common method used to install such covers.



Fig- 41: Method for coating solar panels

### 11. Unique selling points and innovation

- Can be used both, as a solar-powered aircraft or as conventional aircraft.
- Efficient and cost-effective VTOL solution.
- Simple and rugged design suitable for operating at semi-prepared remote locations.
- Autorotation through the use of rotors can prevent damage to aircraft as well as its payload.
- Tricycle landing gear for landing on uneven surfaces.
- Pitch, yaw, and roll control during hover through tiltrotor eliminates the need for a separate reaction control system to balance the aircraft in VTOL mode.

- Payload can also be airdropped easily with minimum human interference with appropriate modifications.

### 12. Different flight modes

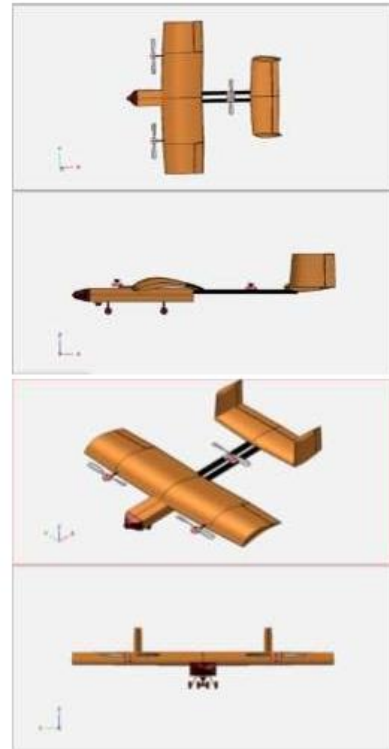


Fig- 42: Helicopter mode

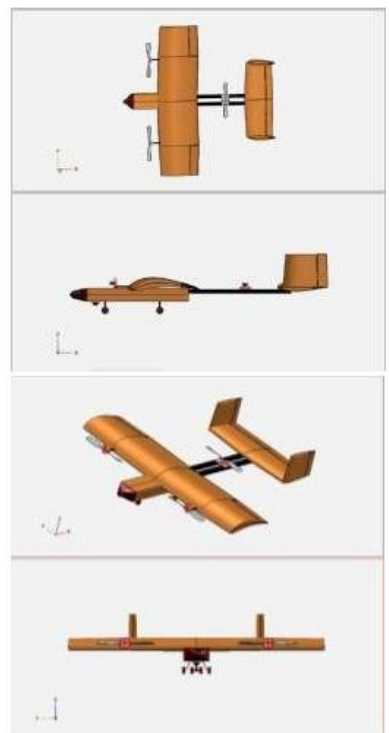


Fig- 43: Flight mode

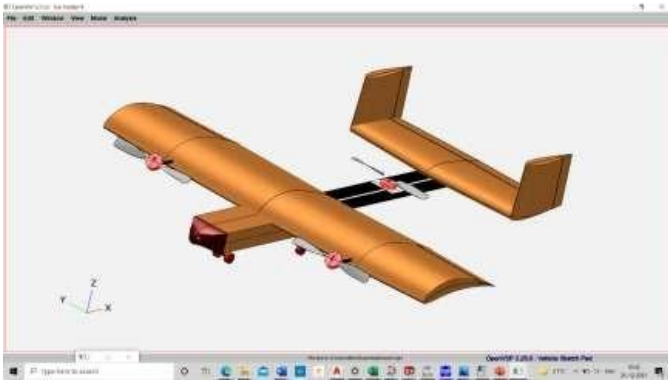


Fig- 44: Transition Phase

### 13. Surveillance area diagram

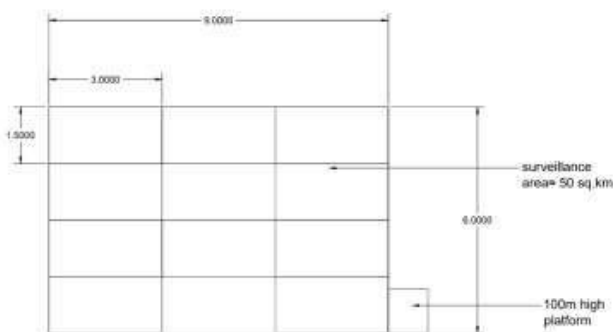


Fig- 45: Surveillance area diagram

### 14. Possible mission plan

- Warm up and accelerate to climb speed in 90 seconds.
- Take off from 100m platform up to 700m at 5 m/s in the helicopter mode in next 4 minutes
- Transition from helicopter mode to flight mode in 30 seconds.
- Acceleration to cruise speed of 14m/s and travel 9km forward in surveillance pattern in next 15 minutes.
- Approximately 11km traveled at a maximum displacement from take-off
- Travel the area of 50km<sup>2</sup> in surveillance pattern.
- Approximately 30 km traveled in total at the end of the cruise in 60 minutes
- Deceleration in next 1.5-2 km in next 5 minutes.
- Transition to helicopter mode and descend at 4 m/s from 700m to 100m platform in next 2 minutes.
- Land on the 100 m platform before 90 minutes.
- Battery replacement (if required)
- And take off for a new mission.

### 15. Conclusion

A tricopter prototype of tilt-rotor UAV configuration has been created for portability and operational processes visible in small diameter areas. Particularly in comparison to certain other tilt-rotor UAVs like TURAC and FireFLY 6, the tilt-rotor UAV employs a different alignment of its front rotors,

that decreases the number of actuators. Compared to the Panther and mini Panther, the proposed UAV tilt-rotor is more compact and portable. The combination of solar energy in UAVs can extend the duration of the flight; therefore, it has the potential to allow for a wider range of UAV applications.

### REFERENCES

1. Oettershagen, P.; Melzer, A.; Mantel, T.; Rudin, K.; Stastny, T.; Wawrzacz, B.; Hinzmann, T.; Leutenegger, S.; Alexis, K.; Siegwart, R. Design of small hand-launched solar-powered UAVs: From concept study to amultidayworld endurance record flight. *J. Field Robot.* 2017, 34, 1352–1377.
2. Morton, S.; D’Sa, R.; Papanikolopoulos, N. Solar Powered UAV: Design and Experiments. In *Proceedings of the IEEE/RSJ International Conference on Intelligent Robots and Systems (IROS)*, Hamburg, Germany, 28 September–3 October 2015
3. Safyanu, B.; Abdullah, M.; Omar, Z. Review of Power Device for Solar-Powered Aircraft Applications. *J. Aerosp. Technol. Manag.* 2019, 11, 4119
4. Emery, K.A. Photovoltaic efficiency measurements—Overview. In *Proceedings of the SPIE—The International Society for Optical Engineering*, Denver, CO, USA, 3 November 2002.
5. Saeed AS, Younes AB, Islam S, et al. A review on the platform design, dynamic modeling, and control of hybrid UAVs. In: 2015 international conference on unmanned aircraft systems (ICUAS) (ed K Valavanis), Denver, CO, USA, 9–12 June 2015, pp. 806–815. IEEE.
6. Carlson S. A hybrid tricopter/flying-wing VTOL UAV. Reston: American Institute of Aeronautics and Astronautics, 2014.
7. Safyanu BD; Abdullah MN; Omar Z (2019) Review of Power Device for Solar-Powered Aircraft Applications. *J Aerosp Technol Manag*, 11
8. <https://aerocad2.com/10-approaches-used-for-solar-powered-airplanes/#:~:text=Solar%20Powered%20Aircraft%201%201%20Pathfinder%20When%20the,Zephyr%20...%208%208.%20S%20ky-Sailor%20...%20More%20items>
9. <https://www.jetir.org/view?paper=JETIREU06010>
10. [https://www.researchgate.net/publication/50946312\\_SOLAR\\_POWER\\_THE\\_FUTURE\\_OF\\_AVIATION\\_INDUSTRY](https://www.researchgate.net/publication/50946312_SOLAR_POWER_THE_FUTURE_OF_AVIATION_INDUSTRY)
11. <https://www.oxfordsaudia.com/en/blog/solar-powered-airplanes-the-history-and-future-of-solar-flights/>
12. <https://www.scielo.br/j/jatm/a/5SVDg4tSPpswhc8P6CscJNv/>
13. [http://sky-sailor.ethz.ch/docs/Conceptual\\_Design\\_of\\_Solar\\_Powered\\_Airplanes\\_for\\_continuous\\_flight2.pdf](http://sky-sailor.ethz.ch/docs/Conceptual_Design_of_Solar_Powered_Airplanes_for_continuous_flight2.pdf)